Chemistry Europe
European Chemical Societies Publishing

Design and Synthesis of New Withaferin A Inspired Hedgehog Pathway Inhibitors

Elisa Bonandi,[a] Mattia Mori,[b] Paola Infante,[c] Irene Basili,[d] Lucia Di Marcotullio,[d, e] Andrea Calcaterra,[f] Federica Catti,[g] Bruno Botta,[f] and Daniele Passarella*[a]

Abstract: Withanolides constitute a well-known family of plant-based alkaloids characterised by widespread biological properties, including the ability of interfering with Hedgehog (Hh) signalling pathway. Following our interest in natural products and in anticancer compounds, we report here the synthesis of a new class of Hh signalling pathway inhibitors, inspired by withaferin A, the first isolated member of withanolides. The decoration of our scaffolds was rationally supported by *in silico* studies, while functional evaluation revealed promising candidates, confirming once again the importance of natural products as inspiration source for the discovery of novel bioactive compounds. A stereoselective approach, based on Brown chemistry, allowed the obtainment and the functional evaluation of the enantiopure hit compounds.

Introduction

Natural products have historically played a key role in the drug discovery process, and nowadays several therapeutic agents display a "natural" origin.[1–4] Thus, despite the advent of high-throughput screening techniques, natural products could still be a prolific source of inspiration for the design of new drug candidates. In this context, this work was inspired by withanolides. Withanolides are a wide family of secondary metabolites found in plants belonging the *Solanaceae* genera, such as *Withania somnifera*, and are structurally characterised by an ergostane-like steroid moiety and a lactone (or a lactone derivative) unit. They display a great pharmacological potential, that includes adaptogenic, diuretic, cytotoxic, sedative, anti-inflammatory and immunomodulatory properties, as well as the ability of crossing the blood brain barrier.[5,6] In fact, the *Withania somnifera* extract has been used for centuries in the ayurvedic medicine and is currently marketed as food supplement. Moreover, some withanolides such as withaferin A (the first member of this family to be isolated), 27-deoxywithaferin A, 24-5,6-deoxywithaferin A and 2,3-dihydro-3-β-O-sulfate withaferin A, possess an interesting anticancer activity, resulting from the simultaneous targeting of different signalling pathways, including Hh signalling pathway.[7] Withanolides are structurally complex molecules, but in 2015 Waldmann demonstrated that some simplified analogues, lacking the steroid moiety, still displayed interesting bioactive properties, being able to inhibit the Smoothened (Smo) protein, one of the key players in Hh signalling.[8]

The ability of interfering with Hh renders withanolides appealing compounds indeed, considering the well-known relationship between Hh aberrant activation and cancer. The Hh signalling is highly conserved in nature,[9] and members of this family of intercellular signalling proteins have been identified as fundamental mediators during the embryonic development in vertebrates and invertebrates.[10,11] Even though the signalling is usually silenced in the adult age in the majority of tissues, it has been demonstrated that its abnormal activation is related to Gorlin syndrome and different cancer types, including basal cells carcinoma (BCC), medulloblastoma, rhabdomyosarcoma, meningiomas, lung, breast, pancreas and ovarian carcinomas.[12–17] Moreover, Hh aberrations play a key role in

[a] *Dr. E. Bonandi, Prof. Dr. D. Passarella*
Department of Chemistry, Università degli Studi di Milano
Via Golgi 19, 20133 Milan (Italy)
E-mail: daniele.passarella@unimi.it
Homepage: https://users.unimi.it/passalab/

[b] *Dr. M. Mori*
Department of Biotechnology, Chemistry and Pharmacy
Università degli Studi di Siena
Via Aldo Moro 2, 53100 Siena (Italy)

[c] *Dr. P. Infante*
Istituto Italiano di Tecnologia
Viale Regina Elena 291, 00161 Rome (Italy)

[d] *Dr. I. Basili, Prof. Dr. L. Di Marcotullio*
Department of Molecular Medicine, University La Sapienza, Roma
Viale Regina Elena 291, 00161 Roma (Italy)

[e] *Prof. Dr. L. Di Marcotullio*
Laboratory affiliated to Istituto Pasteur Italia-Fondazione Cenci Bolognetti,
Department of Molecular Medicine, University La Sapienza
Viale Regina Elena 291, 00161 Roma (Italy)

[f] *Dr. A. Calcaterra, Prof. Dr. B. Botta*
Department of Chemistry and Technology of Drugs
University La Sapienza, Roma, Italy
Piazzale Aldo Moro 5, 00185 Rome (Italy)

[g] *Dr. F. Catti*
Arkansas State University, Campus Querétaro
Carretera Estatal 100, km 17.5. C.P. 76270
Municipio de Colón, Querétaro (México)

Supporting information for this article is available on the WWW under https://doi.org/10.1002/chem.202100315

cancer stem cells (CSCs) proliferation.[18–20] Therefore, Hh signalling inhibition emerged as an extraordinary important target in anticancer therapy, due to the blockage of expression of the genes responsible for tumorigenesis.

The key players in the transduction process are essentially four: the Hh ligands, the Patched receptor (Ptch1, a transmembrane protein including the binding site for the Hh ligands), the G-coupled receptor like protein Smo (the key signal transducer), and three zinc-finger transcription factors (GLIs), inducing the expression of the Hh target genes.[21,22]

Ideally, the inhibition of even one of these key regulators should block the signal transduction. In the last years, research efforts were oriented mainly toward the targeting of Smo,[23] due to the elucidation of the structural determinants involved in Hh activation,[24–26] that allowed the application of *in-silico* techniques to the design of possible antagonists. Several Smo antagonists are currently ongoing clinical trials. Three of them, vismodegib (Erivedge®), sonidegib (Odomzo®) and glasdegib (Daurismo)™ gained the FDA approval for the treatment of metastatic and locally advanced BCC and myeloid leukemia, in 2012, 2015, and 2018, respectively.

The search of new Smo antagonist is still a hot topic in medicine, in particular for the use in combined anticancer therapy, a common strategy to minimize the drug resistance development.

Therefore, combining our interest in natural products, cancer stem cells targeting[20,27] and Hh signalling inhibition,[23,28–37] here we propose the rational design and synthesis of a new class of potential withanolides-inspired Smo inhibitors.

Results and Discussion

Rational design

The design of our target inhibitor **1** was inspired by withaferin A, with the aim of obtaining a class of simplified analogues, easier to be synthesised and still able to interfere with Hh signalling.

To this extent, we planned to maintain unchanged the α,β-unsaturated lactone typical of several withanolides, that appears to establish key interactions with Smo protein. This moiety was decorated with a simple polycyclic framework, able to occupy the narrow antagonists site within Smo, giving additional stabilizing interactions. We came out with a bicyclic carbamate, that replaced the steroid portion of withaferin A. The two key moieties were then connected through a methylene bridge (Figure 1A). Computational studies confirmed that **1**, despite being smaller than withaferin A, is still able to fit the ligand binding site in Smo (Figure 1B). In fact, molecular docking suggested that **1** maintains the typical interactions with Gln472 and Asn219 exerted by the α,β-unsaturated lactone, and establishes additional H-bond interactions with Arg400 through the carbonyl group of the bicyclic carbamate.

Structure **1** is characterized by three stereocentres, and so exists as four couples of enantiomers, that are expected to inhibit Hh signalling to different extents. Therefore, we first prioritized the obtainment of the four racemic compounds, to establish the feasibility of the synthetic strategy and to evaluate the possible bioactivity in a preliminary stage; then, the stereoselective synthesis of the active compounds was achieved.

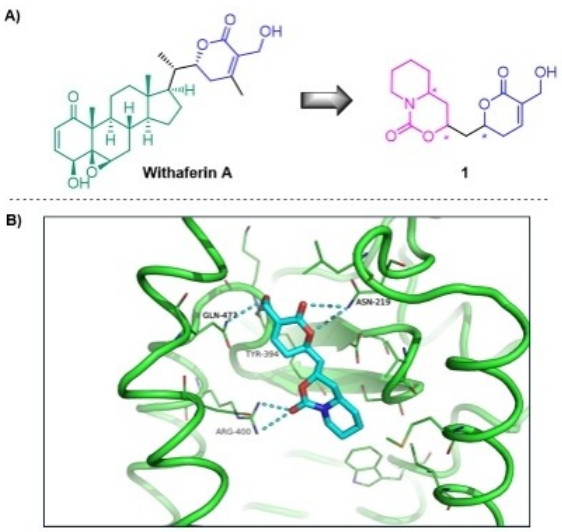

Figure 1. Rational design of scaffold **1**, displaying in blue the common structural features with withaferin A (A); docking pose of **1** in Smo binding site (B).

Synthesis

Once designed our target molecule **1**, the first synthetic strategy we considered foresaw the formation of the carbamate at an early stage of the route and the introduction of the lactone as one of the last steps (Scheme 1). Homoallylic alcohol **2**, previously accessed in our laboratory in all its four stereoisomers, starting from the inexpensive 2-piperidine ethanol, was identified as a promising building block.[38] The employment of Brown's chemistry for the two alkylation steps should allow the control over the stereochemical outcome of the synthesis. In fact, using the proper combination of the two enantiomers of allyl- $Bipc_2$, all the eight stereoisomers of **1** could be potentially

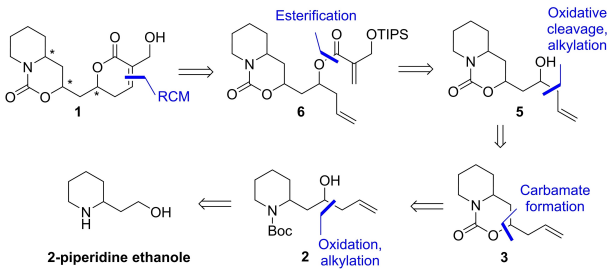

Scheme 1. First retrosynthetic strategy for the synthesis of **1**.

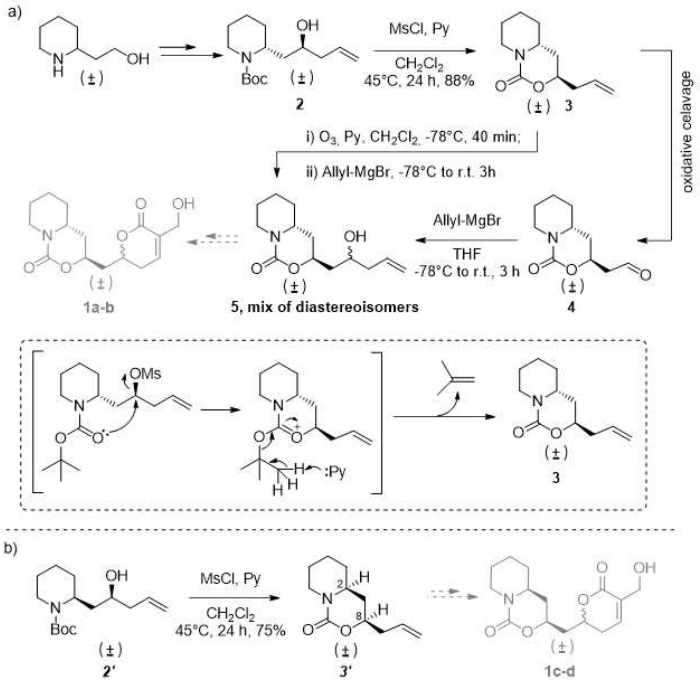

Scheme 2. a) Synthesis of homoallylic alcohol **5**, as mixture of diastereomers, potentially exploitable for the obtainment of stereoisomers **1 a** and **1 b**. b) synthesis of carbamate **3'**, useful for the configuration assignation and for the potential obtainment of stereoisomers **1 c** and **1 d**.

obtained. However, the first explorative studies were performed in not-stereoselective conditions, as already mentioned.

Thus, our first attempt started from the racemic *anti*-diastereomer of the homoallylic alcohol **2** (Scheme 2a). **2** was accessed in three steps from 2-piperidine ethanol, involving the protection of the piperidinic nitrogen, oxidation of the alcohol to aldehyde and alkylation with allylmagnesium bromide.[38] Treatment with methanesulfonyl chloride (MsCl) and a base, such as pyridine, converted compound **2** into the desired carbamate **3**. The reaction involved the elimination of a unit of isobutene and occurred one-pot, with inversion of configuration, leading to the final product in a completely diastereoselective fashion (Box in Scheme 2a).[39] The relative configuration was confirmed by ^{1}H-NOESY NMR experiments, performed on **3** and its *syn*-diastereomer **3'**, synthesised in the same way from homoallylic alcohol **2'** (Scheme 2b). The bidimensional experiment evidenced a cross-peak between protons H_2 and H_8 in the carbamate generated from **2'**, while no cross-peaks were appreciable in the other case.

The double bond of **3** was oxidatively cleaved to the corresponding aldehyde **4**, that should have been allylated, leading to the formation of the diastereomeric mixture of alcohols **5** (Scheme 2a).

The oxidative cleavage of **3** double bond proved to be a challenging step, due to the extreme instability of the obtained product **4**. Several conditions were tested, starting from ozonolysis in the presence of either PPh_3 or Me_2S as reducing agents. Notably, this protocol was previously applied on similar compounds, without any stability issue.[38] Unfortunately in this case, the aldehyde tended to quickly decompose and resulted impossible to be purified. We tried to perform the alkylation step immediately after the work-up on the crude aldehyde and we obtained a mixture of the diastereomers of compound **5**, but with a very low yield (10% over ozonolysis and allylation step, Table 1, Entry 1). Therefore, a mixture of catalytic OsO_4 and $NaIO_4$ in the presence of 2,6-lutidine, was tested, hoping that milder oxidative conditions could have been beneficial.[40] Also in that case, the allylation step was immediately performed on crude **4**. Nevertheless, we observed only a slight yield improvement (20% over the two steps, Table 1, Entry 2). We also tried to condense the two steps in one-pot, performing an ozonolysis in the presence of pyridine, and adding the Grignard's reagent to the reaction mixture, upon alkene consumptions,[41] but the yield was again unsatisfactory (23%, Table 1, Entry 3). Similar stability issues were observed during the oxidative cleavage of compound **3'**.

The impossibility of achieving satisfactory yields over the oxidative cleavage/allylation sequence prompted us to modify the synthetic strategy. In particular, it was decided to create

Table 1. Screening of reaction condition for the oxidative cleavage of **3**.

Entry	Oxidizing agent	Time	Allylation Step	Yield for 5[a]
1	O_3, Me_2S or PPh_3	0.5 h under O_3, 2 h with red. agent	Allyl-MgBr on crude **4**	10%
2	OsO_4, $NaIO_4$	2 h	Allyl-MgBr on crude **4**	20%
3	O_3, Py	40 min	Allyl-MgBr, one pot	23%

[a] Yield calculated over the sum of the two **5** diastereomers.

firstly the lactone motif and to postpone the formation of the bicyclic carbamate at the end of the route, as depicted in Scheme 3.

The key intermediate in this strategy was **8**, that could be synthesised in three steps from **2**,[42] and possesses an homoallylic alcohol convertible into the α,β-unsaturated lactone in two steps, while the piperidine nitrogen and the secondary alcohol on C8 could be exploited to build the carbamate with the same procedure used for **3** synthesis.

For our first efforts, intermediate **2** was exploited once again as starting material. Its hydroxyl group was protected as *tert*-butyldimethylsilyl ether and the double bond underwent oxidative cleavage. In this case, ozonolysis efficiently gave the desired aldehyde, suggesting that the problems relative to the oxidative cleavage of **3** might result from the instability of the carbamate under oxidative conditions. Aldehyde **7** was alkylated in the presence of allylmagnesium bromide, giving the two separable racemic diastereomers **8a** and **8b**, in almost 1:1 ratio. The relative configuration of the newly formed stereocentre was confirmed upon comparison with the previously reported total synthesis of (−)-anaferine, in which the reaction was performed in a stereoselective fashion.[42] The racemic product composed by the couple of (*R,R,R*)- and (*S,S,S*)-enantiomers is indicated as **8a**, and the same nomenclature will be used also for the following intermediates of the synthetic pathway. On the other hand, the other homoallylic alcohol (composed by (*R,R,S*)-and (*S,S,R*)-enantiomers) is indicated as **8b**. The two diastereomers were easily separated through column chromatography and both of them underwent the same synthetic route (Scheme 4a), involving as subsequent step the condensation with carboxylic acid **9**,[8] accessing esters **10a–b**.

The following ring closing metathesis (RCM) proved to be quite challenging and required the screening of three different catalysts, to optimize the formation of the ring-enclosed product. The screening was performed on compound **10a** and the first tested catalyst was the M73-SIMes, a catalysts of choice in several analogous reactions performed in our laboratory, due to its impressive activity even at very low loadings.[42,43] However, in that case we observed a mixture of products, including the desired ring-enclosed compound **11a** and an unsolvable mixture of cross-metathesis (CM) products on the less hindered alkene. Therefore, we tested the 2nd generation Hoveyda-Grubbs catalyst, and a 10-fold dilution. In that case, only a limited amount of the CM dimer was appreciable, but

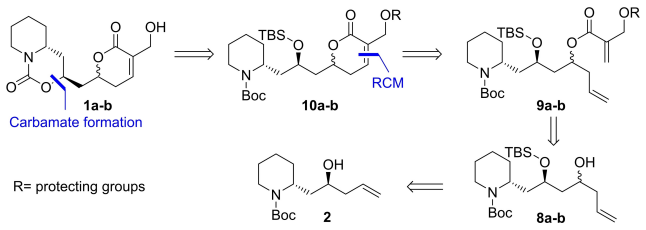

Scheme 3. Final retrosynthetic pathway, reported for clarity sake on the stereoisomers **1a** and **1b**.

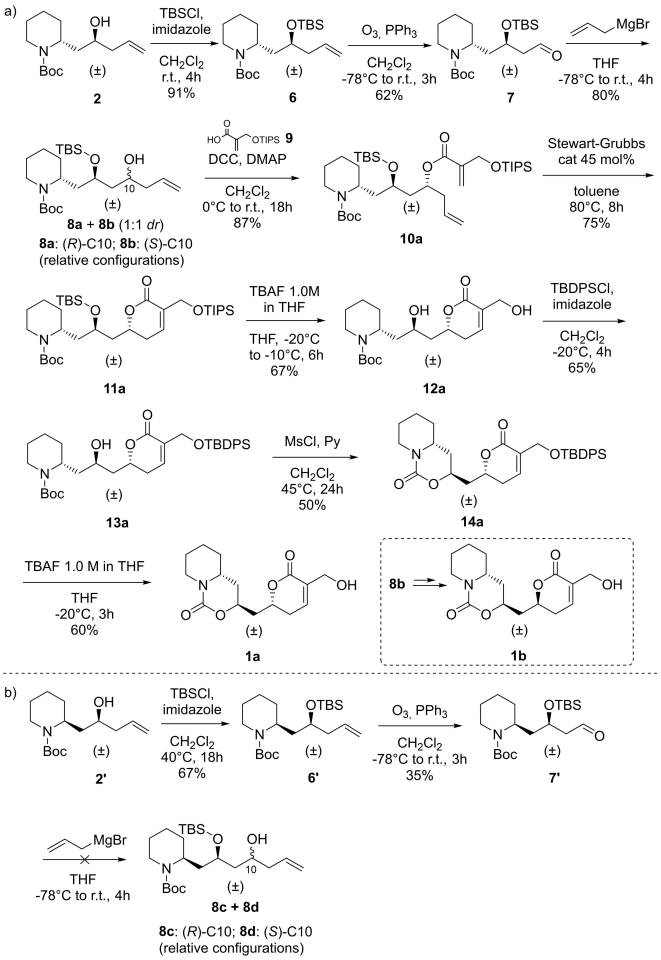

Scheme 4. a) Final synthetic pathway leading to compounds **1a–b**. The reactions are reported on stereoisomers "a" for clarity sake, but the same approach was applied on the homoallylic alcohol **8b**. b) Failed synthetic attempts toward the synthesis of **1c–d**.

the prolonged reaction time required the addition of aliquots of fresh catalyst, to compensate the amount degraded at high temperature. The best results were achieved with the Stewart-Grubbs catalyst, which is a less hindered version of the Hoveyda-Grubbs II, particularly suitable for RCM reactions on bulky alkenes.[8] In this way **11a** was obtained with a satisfactory 75% yield, although using the same sub-stoichiometric amount of catalyst of the previous experiment. Notably, the optimised procedure was applied to the stereoisomer **10b**, giving **11b** with comparable yield.

Once accessed compounds **11a–b**, the two silylethers were cleaved and the primary alcohol was selectively re-protected with the bulky *tert*-butyldiphenylsilyl ether, affording products **13a–b**. Despite the presence of two hindered six-membered rings around the secondary alcohol, it tended to be partially protected as well, so the use of a sub-stoichiometric amount of TBDPSCl (0.9 eq) and low temperature (−20 °C) were essential requirements to gain a good selection over the primary alcohol.

Compounds **13a–b** underwent the diastereoselective cyclisation in the presence of MsCl and pyridine, affording the

bicyclic carbamates **14a**–**b**. To our delight, after the cleavage of the TBDPS protecting group, the final racemic compounds **1a**–**b** were finally obtained.

The same synthetic approach was applied to compound **2'**, to access the two remaining members of our racemic library **1c**–**d**. (Scheme 4b). We immediately realised that the simple difference in C8 configuration deeply impacted the reactivity. The protection of the secondary alcohol, performed under the previously reported conditions, led only to a limited amount of the desired product, accompanied by a huge amount of unreacted starting material. High excess of TBSCl and heating the reaction mixture at 40 °C, gave compound **6'** in 67% yield. Subsequent ozonolysis reaction afforded aldehyde **7'** in unsatisfactory 35% yield, due to its intrinsic instability. The following allylation reaction was tested on the limited amount of aldehyde accessed from the previous step, revealing additional challenges. In fact, not only the two obtained diastereomers **8c** and **8d** were impossible to be purified, but they were formed as minor components, in a mixture of by-products deriving by degradation. For the aforementioned criticisms, the synthesis of compounds **1c** and **1d** was interrupted.

A preliminary biological evaluation of final compounds **1a** and **1b** and some of the in-route key intermediates was attempted, to explore wider portions of the chemical space.[44] Hence, from the obtained results (see Functional evaluation paragraph), the two active intermediates **13b** and **14b** were identified.

Therefore, the stereoselective synthesis of their enantiopure forms of was considered. To this extent, our synthetic protocol was easily adapted in a stereocontrolled fashion, exploiting Brown's chemistry for the alkylation step, to obtain the two enantiomers of homoallylic alcohol **8b**.

As appreciable in Scheme 5, enantiomer **(+)-8b** ((*R,R,S*)-configuration) was synthesised starting from **(+)-2** ((*R,S*)-configuration),[38] that underwent TBS-protection, oxidative cleavage to aldehyde and stereoselective allylation in the presence of (-)-diisopinocampheylallyl borane.[42] Analogously, **(−)-8b** (*S,S,R*)-configuration) was accessed with 9:1 *dr* (See Supporting Information), starting from **(−)-2** and using (+)-diisopinocampheylallyl borane as allylating agent.

Enantiomers **(+)-8b** and **(−)-8b** underwent the same synthetic pathway depicted in Scheme 4a, to afford the desired compounds **(+)-13b**, **(−)-13b**, **(+)-14b** and **(−)-14b**, that were tested with the same protocols employed for the racemic compounds. The complete results of the functional evaluation of the active compounds are reported in the following paragraph.

Functional evaluation

Preliminary testing on the racemic compounds

The ability of the synthesized compounds to inhibit Hh signalling *in vitro* was investigated by a luciferase reporter assay, which is widely used for characterising Hh antagonists. Racemic compounds **1a** and **1b** were submitted together with some of the previous key synthetic intermediates, to improve the portion of the chemical space explored in this study. NIH3T3 Shh Light II cells (immortalized embryonic fibroblast cell line), stably incorporating a Gli-responsive firefly luciferase (Gli-RE)[45] and the pRL-TK Renilla as normalization control, were treated with the synthetic SMO agonist SAG,[46] alone or in combination with selected compounds at the concentrations of 5,10,20 μM.

1a and **1b** resulted inactive at the luciferase assay, while **13b** and **14b** (Figure 2A and 2B) revealed high activity as Hh inhibitors, with an IC_{50} of 7.44 μM and 12.95 μM, respectively.

The activity of compound **14b** supports the computational studies and confirms the relevance of the designed scaffold. The lack of activity of **1b** sounds surprising in a first instance, if

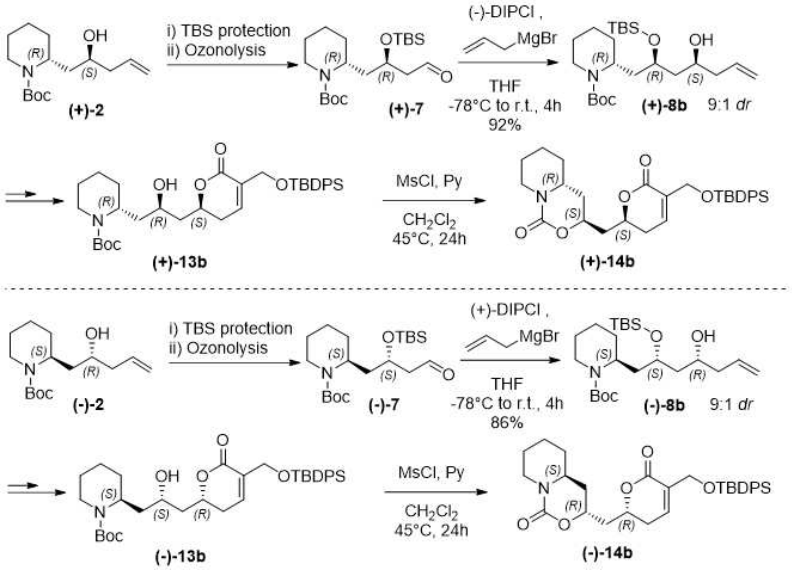

Scheme 5. Stereoselective synthesis of the enantiomers of compounds **13b** and **14b**.

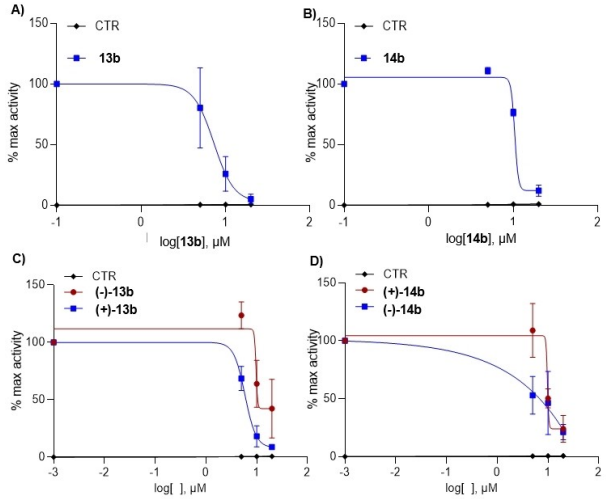

Figure 2. Inhibitory effects of **13b** and **14b** and the selected enantiomers on Hh signalling activity. The dose-response curve in SAG-treated NIH3T3 Shh-Light II cells treated for 48 h with the increasing concentrations of compounds **13b** (**A**), **14b** (**B**), (+)-**13b** and (−)-**13b** (**C**), (+)-**14b** and (−)-**14b** (**D**). Data show the mean ± S.D. of three independent experiments. (*) $p < 0.05$; (**) $p < 0.01$; (***) $p < 0.001$ *vs* SAG.

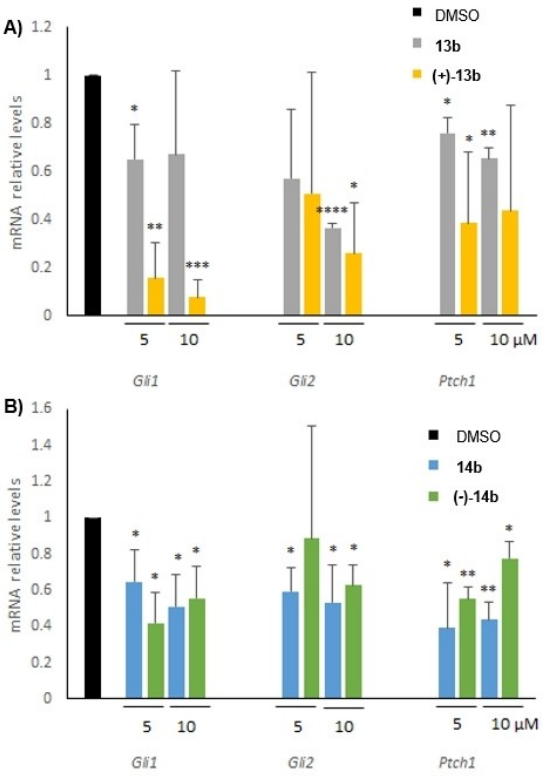

Figure 3. Inhibitory effect of compounds **13b**, **14b**, (+)-**13b**, and (−)-**14b** on Hh-active cell model Ptch1$^{-/-}$ MEFs. The graphs show mRNA expression levels of *Gli1*, *Gli2*, and *Ptch1* in Ptch1$^{-/-}$ MEFs treated for 48 h with DMSO as a control, or the compounds **13b** and (+)-**13b** (**A**), or **14b** and (−)-**14b** (**B**) at the final concentrations of 5 and 10 μM. Hh target genes mRNA levels were determined by qRT-PCR normalized to endogenous controls *β2-microglobulin* and *Hprt*. Data show the mean ± S.D. of three independent experiments. (*) $p < 0.05$; (**) $p < 0.01$; (***) $p < 0.001$; (****); $p < 0.0001$ *vs* DMSO.

compared with its protected version **14b**. However, this behaviour could derive from the diverse polarity of **1b** and **14b**, resulting in a different ability in overcoming the cellular barrier or even in a completely different interaction with membrane transporters.

Evaluation of the enantiopure forms of the active intermediates as Hh inhibitors

Intermediates **13b** and **14b** were synthesised in an enantioselective fashion, and the inhibitory effect of the single enantiomers was evaluated analogously to the racemic compounds. The results of luciferase assays showed that (+)-**13b** inhibited Gli1 transcriptional activity better than (−)-**13b**, with IC_{50} of 6.379 μM and 16.5 μM, respectively (Figure 2C). On the other hand, (−)-**14b** demonstrated a stronger inhibitory effect ($IC_{50} = 6.568$ μM) than its enantiomer (+)-**14b** ($IC_{50} = 11.33$ μM) (Figure 2D).

To further prove the capability of the most active compounds to target Hh signalling, we used the Hh-active cell model Ptch1$^{-/-}$ mouse embryonic fibroblasts (Ptch1$^{-/-}$ MEFs), in which the deletion of the inhibitory Ptch1 receptor releases Smo function and leads to a constitutive activation of Gli transcription factors.[47] Ptch1$^{-/-}$ MEFs were treated for 48 h at 5 and 10 μM with the racemates **13b** and **14b**, and their most active enantiomers, (+)-**13b** and (−)-**14b**, respectively. The treatment with (+)-**13b** reduced the mRNA levels of *Gli1* (the final effector of the Hh signalling), *Ptch1*, and *Gli2* strongly than compound **13b**, used at the same concentrations (Figure 3A). Instead, **14b** and (−)-**14b** showed a similar effect to each other on the reduction of Hh target genes expression levels (Figure 3B). These data sustain the ability of the selected compounds to inhibit the Hh signalling and identify compound **13b** and its enantiomer (+)-**13b** as the most effective Hh-inhibitors among the ones we have tested.

Computational studies

The predicted binding mode of **13b** and **14b** isolated enantiomers was investigated by structure-based computational modelling tools including molecular docking, energy minimization and scoring with XSCORE. Taking advantage of available crystallographic structures of the human Smo receptor in complex with antitumor an agent,[24] the conformational fitting of (+)-**13b**, (−)-**13b**, (+)-**14b** and (−)-**14b** in the Smo antagonists site was predicted by docking with OEDocking (OpenEye Scientific Software).[48] Top-scoring poses were then relaxed by energy minimization, while ligands theoretical affinity was computed as a -pK_d value by the XSCORE function.[49] Results unequivocally show that all compounds are able to fit the antagonists site, with the bulky TBDPS protecting group occupying its upper portion in correspondence of the extracellular region of the Smo receptor (Figure 4).

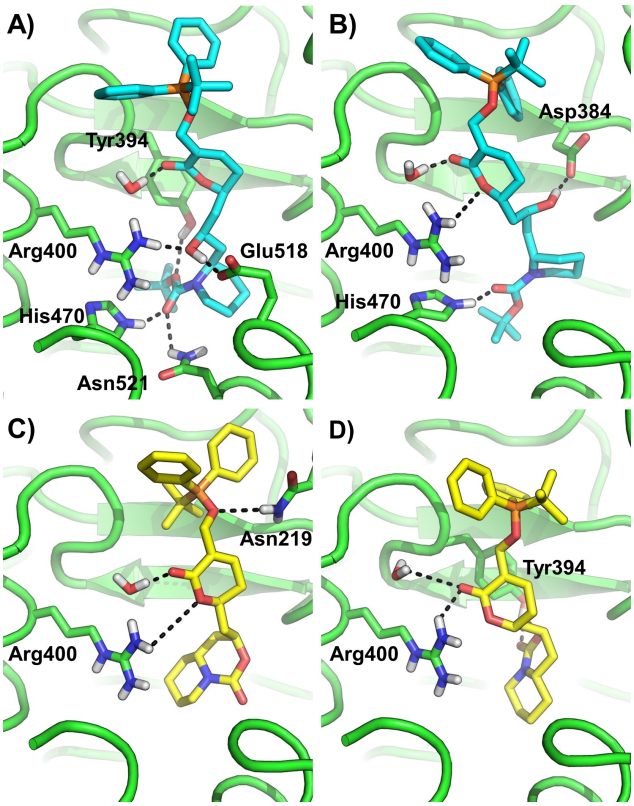

Figure 4. Predicted binding mode of compounds (+)-**13b** (A), (−)-**13b** (B), (+)-**14b** (C), and (−)-**14b** (D) within the crystallographic structure of the Smo receptor. The protein is shown as cartoon. Small molecules and residues contacted by H-bond interactions including the crystallographic water molecule are shown as sticks. (+)-**13b** and (−)-**13b** enantiomers are coloured cyan. (+)-**14b** and (−)-**14b** enantiomers are coloured yellow. H-bond interactions are highlighted a black dashed lines. Residues contacted by H-bonds are labelled.

This binding mode is consistent with the narrow shape of the antagonists site, as underlined by structural and computational studies.[23,35,50]

Moreover, a remarkable overlapping between the predicted binding mode of our compounds and the crystallographic pose of a Smo antagonist endowed with antitumor activity was observed, showing that the TBDPS group occupies the same position as the fluorobenzoyl moiety of the reference Smo antagonist (Supporting Information, Figure S2).

In details, all compounds still establish the key H-bond interaction with Arg400, a crucial residue in the binding to Smo antagonists,[51] and with a crystallographic water molecule that was characterized by X-ray crystallography studies. In addition, small molecules are H-bonded to residues such as Asn219, Asp384, Tyr394, His470, and Glu518 as depicted in Figure 4. It is worth noting that in **13b** H-bonds are performed also by atoms from the Boc protecting group, while comparison between the predicted binding mode and functional data of **1** and **14b** suggests that the TBDPS protecting group (also installed in **13b**) favourably impacts on the ligand's affinity to Smo, most likely due to hydrophobic interactions with residues in the upper part of the Smo antagonists site. Among the test set, (+)-**13b** is able to establish an extensive network of H-bond interactions, whereas the other tested derivatives perform worst in this respect. Notably, scoring analysis suggests that this binding peculiarity of (+)-**13b** is associated to a higher theoretical affinity compared to other compounds studied in this work (See Supporting Information). This is remarkably in agreement with experimental data, which corroborate structural data depicted by computational modelling.

Notably, docking simulations revealed the presence of a cysteine residue within the ligand binding site (*i.e.* Cys469), that could in principle interact with the α,β-unsaturated lactone of our inhibitors. In fact, withanolides, and in particular withaferin A, are well-known for eliciting their multiple biological activities through the formation of covalent Michael-like interactions with cysteine residues.[52–55] To rule out this possibility, the reactivity of our inhibitors toward the Michael addition of thiol-containing moieties (such as glutathione and benzyl mercaptan) was evaluated. However, no formation of Michael adducts was detected by mass spectrometry analysis when each thiol compound was added to **13b**, **14b**, or **1b** in a 1:1 ratio. These results are in agreement with the work by Gunatilaka *et al.*, indicating that Withaferin A interacts with *N*-acetylcysteine at the level of its enone ring (a motif that is not considered in our design strategy), and not at the lactone portion, which was incorporated into our scaffolds.[55] Finally, evidence of non-covalent interaction of our derivative with the Smo receptor supports the binding hypothesis and molecular modelling outcomes, further excluding the possibility of unspecific interactions with cysteine residues of Smo or other unrelated targets.

Conclusion

In summary, the structure of withaferin A and its activity in inhibiting the Hh pathway moved us to design a simplified compound that resulted a synthetic challenge. An efficient synthesis that presents as key steps a RCM and two allylation reactions is described. The stereoselective approach is based on asymmetric Brown allylation. The functional evaluation identified two active compounds. Compound **13b** differs from the designed target for the absence of the carbamate containing ring, for the presence of a further hydroxyl group and a lipophilic protecting group on the primary alcohol, while **14b** presents a lipophilic group instead of the hydroxy group on the dehydrolactone ring. These results further demonstrate: a) the importance of natural products in inspiring the discovery of new relevant scaffolds and permitting a wider exploration of the chemical space; b) the efficacy of computational studies in drug design, and c) the importance of the functional evaluation of the synthetic intermediates to better sample the chemical space surrounding the designed structure. The difference in the detected activity for structurally close compounds will guide us in further exploration of the Hh inhibitors chemical space.

Acknowledgements

The authors express their gratitude to Ministero dell'Istruzione dell'Università e della Ricerca for the Project 20175XBSX4_003 and 2017BF3PXZ (**Prin2017**), Associazione Italiana per la Ricerca sul Cancro Grants #IG20801; Progetti di Ricerca di Università Sapienza di Roma; Dipartimenti di Eccellenza - L. 232/2016; Pasteur Institute/Cenci Bolognetti Foundation; Istituto Italiano di Tecnologia (IIT). Authors wish to thank the OpenEye Free Academic Licensing Programme for providing a free academic licence for molecular modelling and chemoinformatics software

Conflict of Interest

The authors declare no conflict of interest.

Keywords: 2-piperidine ethanol · Hedgehog inhibitors · Hedgehog signalling pathway · natural products · withaferin A

[1] F. E. Koehn, G. T. Carter, *Nat. Rev. Drug Discovery* **2005**, *4*, 206–220.
[2] D. J. Newman, G. M. Cragg, *J. Nat. Prod.* **2016**, *79*, 629–661.
[3] A. L. Harvey, *Drug Discovery Today* **2008**, *13*, 894–901.
[4] F. Ghirga, D. Quaglio, M. Mori, S. Cammarone, A. Iazzetti, A. Goggiamani, C. Ingallina, B. Botta, A. Calcaterra, *Org. Chem. Front.* **2021**, *8*, 996–1025.
[5] P. T. White, C. Subramanian, H. F. Motiwala, M. S. Cohen, Eds.: S. C. Gupta, S. Prasad, B. B. Aggarwal, Springer International Publishing, *Anti-inflammatory Nutraceuticals and Chronic Diseases***2016**, pp. 329–373.
[6] G. Kumar, R. Patnaik, *Med. Hypotheses* **2016**, *92*, 35–43.
[7] T. Yoneyama, M. A. Arai, S. K. Sadhu, F. Ahmed, M. Ishibashi, *Bioorg. Med. Chem. Lett.* **2015**, *25*, 3541–3544.
[8] J. Švenda, M. Sheremet, L. Kremer, L. Maier, J. O. Bauer, C. Strohmann, S. Ziegler, K. Kumar, H. Waldmann, *Angew. Chem. Int. Ed.* **2015**, *54*, 5596–5602; *Angew. Chem.* **2015**, *127*, 5688–5694.
[9] Y. Jia, Y. Wang, J. Xie, *Arch. Toxicol.* **2015**, *89*, 179–191.
[10] P. W. Ingham, *Genes Dev.* **2001**, *15*, 3059–3087.
[11] Y. Echelard, L. Shen, B. St-Jacques, J. A. McMahon, A. P. McMahon, D. J. Epstein, J. Mohler, *Cell* **1993**, *75*, 1417–1430.
[12] E. H. Epstein, *Nat. Rev. Cancer* **2008**, *8*, 743–754.
[13] V. E. Clark, E. Z. Erson-Omay, A. Serin, J. Yin, J. Cotney, K. Ozduman, T. Avsar, J. Li, P. B. Murray, O. Henegariu, S. Yilmaz, J. M. Gunel, G. Carrion-Grant, B. Yilmaz, C. Grady, B. Tanrikulu, M. Bakircioglu, H. Kaymakcalan, A. O. Caglayan, L. Sencar, E. Ceyhun, A. F. Atik, Y. Bayri, H. Bai, L. E. Kolb, R. M. Hebert, S. B. Omay, K. Mishra-Gorur, M. Choi, J. D. Overton, E. C. Holland, S. Mane, M. W. State, K. Bilguvar, J. M. Baehring, P. H. Gutin, J. M. Piepmeier, A. Vortmeyer, C. W. Brennan, M. N. Pamir, T. Kilic, R. P. Lifton, J. P. Noonan, K. Yasuno, M. Gunel, *Science* **2013**, *339*, 1077–1080.
[14] R. McMillan, W. Matsui, *Clin. Cancer Res.* **2012**, *18*, 4883–4888.
[15] R. L. Johnson, A. L. Rothman, J. Xie, L. V. Goodrich, J. W. Bare, J. M. Bonifas, A. G. Quinn, R. M. Myers, D. R. Cox, E. H. Epstein, M. P. Scott, *Science* **1996**, *272*, 1668–1671.
[16] U. Tostar, C. J. Malm, J. M. Meis-Kindblom, L. G. Kindblom, R. Toftgård, A. B. Undén, *J. Pathol.* **2006**, *208*, 17–25.
[17] D. Amakye, Z. Jagani, M. Dorsch, *Nat. Med.* **2013**, *19*, 1410–1422.
[18] A. A. Merchant, W. Matsui, *Clin. Cancer Res.* **2010**, *16*, 3130–3140.
[19] C. R. Cochrane, A. Szczepny, D. N. Watkins, J. E. Cain, *Cancers* **2015**, *7*, 1554–1585.
[20] P. A. Sotiropoulou, M. S. Christodoulou, A. Silvani, C. Herold-Mende, D. Passarella, *Drug Discovery Today* **2014**, *19*, 1547–1562.
[21] R. T. H. Lee, Z. Zhao, P. W. Ingham, *Development* **2016**, *143*, 367–372.
[22] J. Zhang, X.-J. Tian, J. Xing, *J. Clin. Med.* **2016**, *5*, 41.
[23] F. Ghirga, M. Mori, P. Infante, *Bioorg. Med. Chem. Lett.* **2018**, *28*, 3131–3140.
[24] C. Wang, H. Wu, V. Katritch, G. W. Han, X.-P. Huang, W. Liu, F. Y. Siu, B. L. Roth, V. Cherezov, R. C. Stevens, *Nature* **2013**, *497*, 338–343.
[25] E. F. X. Byrne, R. Sircar, P. S. Miller, G. Hedger, G. Luchetti, S. Nachtergaele, M. D. Tully, L. Mydock-McGrane, D. F. Covey, R. P. Rambo, M. S. P. Sansom, S. Newstead, R. Rohatgi, C. Siebold, *Nature* **2016**, *535*, 517–522.
[26] E. F. Byrne, G. Luchetti, R. Rohatgi, C. Siebold, *Curr. Opin. Cell Biol.* **2018**, *51*, 81–88.
[27] C. Marucci, G. Fumagalli, F. Calogero, A. Silvani, M. Christodoulou, N. Martinet, D. Passarella, *Curr. Pharm. Des.* **2015**, *21*, 5547–5557.
[28] M. S. Christodoulou, M. Mori, R. Pantano, R. Alfonsi, P. Infante, M. Botta, G. Damia, F. Ricci, P. A. Sotiropoulou, S. Liekens, B. Botta, D. Passarella, *ChemPlusChem* **2015**, *80*, 938–943.
[29] P. Infante, A. Malfanti, D. Quaglio, S. Balducci, S. De Martin, F. Bufalieri, F. Mastrotto, I. Basili, M. Garofalo, L. Lospinoso Severini, M. Mori, I. Manni, M. Moretti, C. Nicoletti, G. Piaggio, P. Caliceti, B. Botta, F. Ghirga, S. Salmaso, L. Di Marcotullio, *Cancer Lett.* **2021**, *499*, 220–231.
[30] G. Fumagalli, B. Stella, I. Pastushenko, F. Ricci, M. S. Christodoulou, G. Damia, D. Mazza, S. Arpicco, C. Giannini, L. Morosi, F. Dosio, P. A. Sotiropoulou, D. Passarella, *ACS Med. Chem. Lett.* **2017**, *8*, 953–957.
[31] S. Berardozzi, F. Bernardi, P. Infante, C. Ingallina, S. Toscano, E. De Paolis, R. Alfonsi, M. Caimano, B. Botta, M. Mori, L. Di Marcotullio, F. Ghirga, *Eur. J. Med. Chem.* **2018**, *156*, 554–562.
[32] A. Diukendjieva, M. M. Zaharieva, M. Mori, P. Alov, I. Tsakovska, T. Pencheva, H. Najdenski, V. Křen, C. Felici, F. Bufalieri, L. Di Marcotullio, B. Botta, M. Botta, I. Pajeva, *Antioxidants* **2020**, *9*, 384.
[33] L. Lospinoso Severini, D. Quaglio, I. Basili, F. Ghirga, F. Bufalieri, M. Caimano, S. Balducci, M. Moretti, I. Romeo, E. Loricchio, M. Maroder, B. Botta, M. Mori, P. Infante, L. Di Marcotullio, *Cancers* **2019**, *11*, 1518.
[34] A. Calcaterra, V. Iovine, B. Botta, D. Quaglio, I. D'Acquarica, A. Ciogli, A. Iazzetti, R. Alfonsi, L. Lospinoso Severini, P. Infante, L. Di Marcotullio, M. Mori, F. Ghirga, *J. Enzyme Inhib. Med. Chem.* **2018**, *33*, 349–358.
[35] P. Infante, R. Alfonsi, C. Ingallina, D. Quaglio, F. Ghirga, I. D'Acquarica, F. Bernardi, L. Di Magno, G. Canettieri, I. Screpanti, A. Gulino, B. Botta, M. Mori, L. Di Marcotullio, *Cell Death Dis.* **2016**, *7*, 2376–2376.
[36] D. Quaglio, P. Infante, L. Di Marcotullio, B. Botta, M. Mori, *Expert Opin. Ther. Pat.* **2020**, *30*, 235–250.
[37] L. Lospinoso Severini, F. Ghirga, F. Bufalieri, D. Quaglio, P. Infante, L. Di Marcotullio, *Expert Opin. Ther. Targets* **2020**, *24*, 1159–1181.
[38] C. Marucci, M. S. Christodoulou, S. Pieraccini, M. Sironi, F. Dapiaggi, D. Cartelli, A. M. Calogero, G. Cappelletti, C. Vilanova, S. Gazzola, G. Broggini, D. Passarella, *Eur. J. Org. Chem.* **2016**, *2016*, 2029–2036.
[39] S. Mill, C. Hootelé, *Can. J. Chem.* **1996**, *74*, 2434–2443.
[40] W. Yu, Y. Mei, Y. Kang, Z. Hua, Z. Jin, *Org. Lett.* **2004**, *6*, 3217–3219.
[41] R. Willand-Charnley, P. H. Dussault, *J. Org. Chem.* **2013**, *78*, 42–47.
[42] E. Bonandi, G. Tedesco, D. Perdicchia, D. Passarella, *Molecules* **2020**, *25*, 1057.
[43] E. Bonandi, P. Marzullo, F. Foschi, D. Perdicchia, L. Lo Presti, M. Sironi, S. Pieraccini, G. Gambacorta, J. Saupe, L. Dalla Via, D. Passarella, *Eur. J. Org. Chem.* **2019**, *2019*, 4013–4019.
[44] G. L. Thomas, E. E. Wyatt, D. R. Spring, *Curr. Opin. Drug Discovery Dev.* **2006**, *9*, 700–712.
[45] J. Talpale, J. K. Chen, M. K. Cooper, B. Wang, R. K. Mann, L. Milenkovic, M. P. Scott, P. A. Beachy, *Nature* **2000**, *406*, 1005–1009.
[46] J. K. Chen, *Genes Dev.* **2002**, *16*, 2743–2748.
[47] L. V. Goodrich, L. Milenković, K. M. Higgins, M. P. Scott, *Science* **1997**, *277*, 1109–1113.
[48] M. McGann, *J. Comput.-Aided Mol. Des.* **2012**, *26*, 897–906.
[49] R. Wang, L. Lai, S. Wang, *J. Comput.-Aided Mol. Des.* **2002**, *16*, 11–26.
[50] C. Wang, H. Wu, T. Evron, E. Vardy, G. W. Han, X.-P. Huang, S. J. Hufeisen, T. J. Mangano, D. J. Urban, V. Katritch, V. Cherezov, M. G. Caron, B. L. Roth, R. C. Stevens, *Nat. Commun.* **2014**, *5*, 4355.
[51] H. J. Sharpe, W. Wang, R. N. Hannoush, F. J. de Sauvage, *Nat. Chem. Biol.* **2015**, *11*, 246–255.
[52] Y. Yokota, P. Bargagna-Mohan, P. P. Ravindranath, K. B. Kim, R. Mohan, *Bioorg. Med. Chem. Lett.* **2006**, *16*, 2603–2607.
[53] J. H. Oh, T. J. Lee, J. W. Park, T. K. Kwon, *Eur. J. Pharmacol.* **2008**, *599*, 11–17.
[54] Y. Yu, A. Hamza, T. Zhang, M. Gu, P. Zou, B. Newman, Y. Li, A. A. L. Gunatilaka, C. G. Zhan, D. Sun, *Biochem. Pharmacol.* **2010**, *79*, 542–551.
[55] E. M. K. Wijeratne, Y. M. Xu, R. Scherz-Shouval, M. T. Marron, D. D. Rocha, M. X. Liu, L. V. Costa-Lotufo, S. Santagata, S. Lindquist, L. Whitesell, A. A. L. Gunatilaka, *J. Med. Chem.* **2014**, *57*, 2851–2863.

Manuscript received: February 26, 2021
Accepted manuscript online: April 3, 2021
Version of record online: May 4, 2021

